

**N. M. Porotnikova^{ab*}, E. P. Antonova^{ab},
 A. V. Khodimchuk^{ab}, E. S. Tropin^{ab},
 A. S. Farlenkov^{ab}, M. V. Ananyev^{ab}**

^a *Institute of High Temperature Electrochemistry,
 Ural Branch of Russian Academy of Sciences,
 20 Akademicheskaya St., Ekaterinburg, 620137, Russian Federation*

^b *Ural Federal University,
 19 Mira St., Ekaterinburg, 620002, Russian Federation*

*E-mail: n.porotnikova@mail.ru

Oxygen diffusion and surface exchange kinetics for the mixed-conducting oxide $\text{La}_{0.6}\text{Sr}_{0.4}\text{Co}_{0.8}\text{Fe}_{0.2}\text{O}_{3-\delta}$

Studies of oxygen surface exchange kinetics for $\text{La}_{0.6}\text{Sr}_{0.4}\text{Co}_{0.8}\text{Fe}_{0.2}\text{O}_{3-\delta}$ oxide were performed using the technique of isotopic exchange of molecular oxygen with analysis of gas phase isotopic composition in a static circulation system at the temperatures of 600–800 °C in the oxygen pressure range of 0.27–2.13 kPa. The values of interphase exchange rate and oxygen diffusion coefficient were determined. The effective activation energies for oxygen exchange and diffusion processes as well as the exponents in the dependence of these values versus oxygen pressure in the double logarithmic coordinates were calculated. The process of oxygen dissociative adsorption at the surface of $\text{La}_{0.6}\text{Sr}_{0.4}\text{Co}_{0.8}\text{Fe}_{0.2}\text{O}_{3-\delta}$ oxide was found to be the rate-determining stage.

Keywords: oxygen isotope exchange; oxygen diffusion; lanthanum-strontium cobaltite-ferrite; rate-determining stage

Received: 14.11.2018. Accepted: 11.12.2018. Published: 31.12.2018.

© Porotnikova N. M., Antonova E. P., Khodimchuk A. V., Tropin E. S., Farlenkov A. S., Ananyev M. V., 2018

Introduction

Over the last decades, complex oxides with the perovskite structure based on the lanthanum cobaltite attract much attention as potential cathode materials for solid oxide electrochemical devices [1–4]. Variation of cations concentration in these oxides results in the physicochemical properties changes in the oxide-based materials [5, 6]. Complex oxides with a common formula $\text{La}_{1-x}\text{Sr}_x\text{Co}_{1-y}\text{Fe}_y\text{O}_{3-\delta}$ are among the most perspective cathode materials. A sufficient amount of information available in the literature

has focused on the study of phase equilibria and physicochemical properties of oxides in this system [7–13]. In order to create the effectively operating cathodes based on lanthanum-strontium cobaltite-ferrites, it is vital to understand in detail the oxygen exchange and diffusion mechanisms in these materials.

The main purpose of the present work was to study oxygen diffusion and surface exchange kinetics in $\text{La}_{0.6}\text{Sr}_{0.4}\text{Co}_{0.8}\text{Fe}_{0.2}\text{O}_{3-\delta}$ oxide.

Experimental

The $\text{La}_{0.6}\text{Sr}_{0.4}\text{Co}_{0.8}\text{Fe}_{0.2}\text{O}_{3-\delta}$ oxide was prepared using the citrate-nitrate technology. Lanthanum oxide (LaO-D , 99,99635%), strontium carbonate SrCO_3 (ACS), cobalt nitrate $\text{Co}(\text{NO}_3)_2 \cdot 6\text{H}_2\text{O}$ (chemically pure), iron citrate $\text{C}_6\text{H}_5\text{FeO}_7 \cdot \text{H}_2\text{O}$ (Fluka Analytical) were used as initial reagents. The synthesis was performed at the temperature of 1100 °C for 5 hours.

In order to perform the oxygen isotope exchange measurements, dense ceramic was fabricated. The obtained powders were ground and compacted into the form of disks using 1% water solution of polyvinyl alcohol that served as a bounding agent. The final sintering was performed at the temperature of 1250 °C for 5 hours in air. A relative density of the obtained ceramics was about ~ 92%. Finally, the sintered dense specimens were polished using diamond pastes, such as ACM 7/5 NVMC (Federal Standard 25593–83) and ACM 1/0 NOM (Federal Standard 16377–71).

The phase composition of the $\text{La}_{0.6}\text{Sr}_{0.4}\text{Co}_{0.8}\text{Fe}_{0.2}\text{O}_{3-\delta}$ sample was determined before and after the isotope experiments using a Rigaku D/MAX-2200V diffractometer in the Cu K α emission at room temperature. According to the X-ray analy-

sis, the sample was single phase after synthesis ($R\bar{3}c$ space group, cell parameters $a = 5.4270(4)$ Å, $c = 13.239(2)$ Å) and after completing measurements at high temperatures and low oxygen pressures (Fig. 1), which confirms its stability during long-term tests.

The analysis of the particle size distribution for powder materials was performed by the laser scattering method using a Malvern Mastersizer 2000. To grind the agglomerated particles, the slurry was mixed using a stirrer with the rate of ~2000 rpm, as well as subjected to an ultrasound treatment. Fig. 2 illustrates the volume fraction versus particle size distribution function.

The microphotographs of the ceramics cross-section were made by a scanning electron microscope Tescan MIRA 3. Fig. 3 presents the microphotograph obtained in a beam of back-scattered electrons. The contrast of the images is mainly due to the chemical composition of the studied material surface. As can be seen from Fig. 4, there are small inclusions of cobalt-rich phase at the grains boundaries (probably cobalt oxide); however, the fraction is insignificant, it is less than 0.5%.

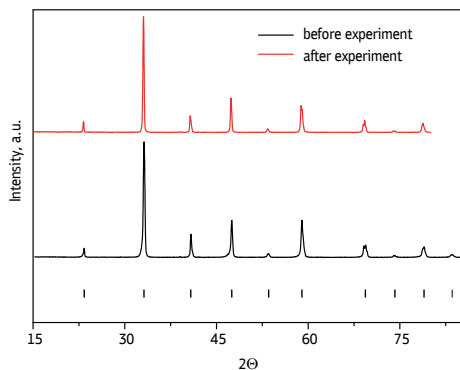


Fig. 1. XRD patterns for $\text{La}_{0.6}\text{Sr}_{0.4}\text{Co}_{0.8}\text{Fe}_{0.2}\text{O}_{3-\delta}$ oxide before and after isotope experiments

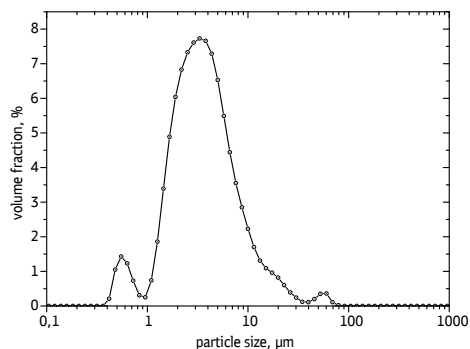


Fig. 2. Particle size distribution function for the $\text{La}_{0.6}\text{Sr}_{0.4}\text{Co}_{0.8}\text{Fe}_{0.2}\text{O}_{3-\delta}$ powder

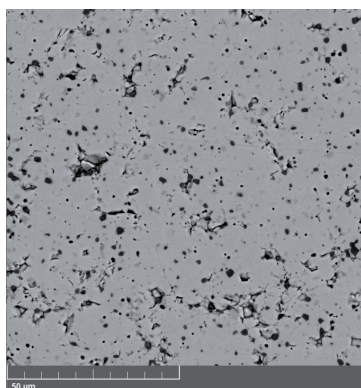


Fig. 3. SEM image of cross-section of $\text{La}_{0.6}\text{Sr}_{0.4}\text{Co}_{0.8}\text{Fe}_{0.2}\text{O}_{3-\delta}$ ceramics in BSE mode

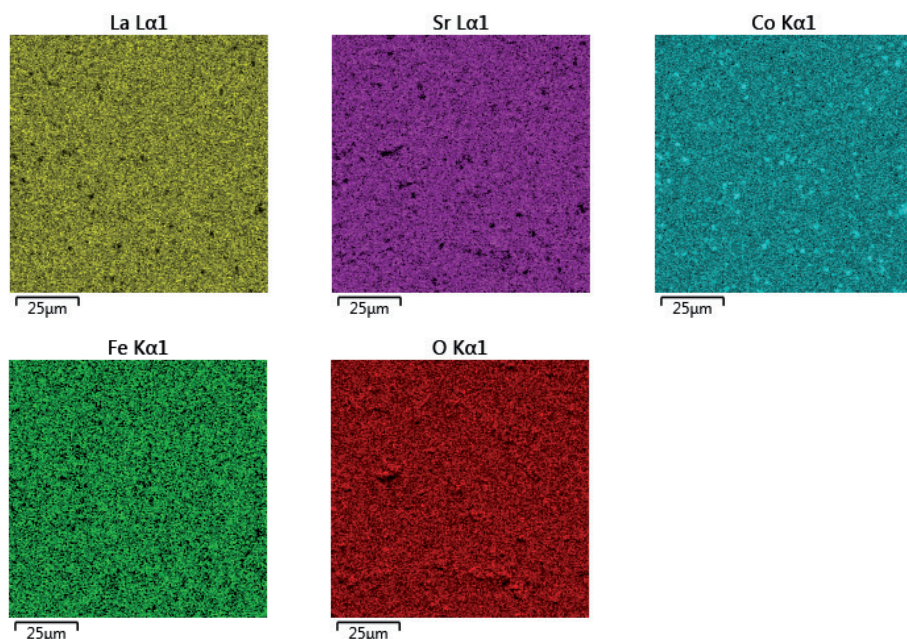


Fig. 4. EDX mapping for $\text{La}_{0.6}\text{Sr}_{0.4}\text{Co}_{0.8}\text{Fe}_{0.2}\text{O}_{3-\delta}$ ceramics

The oxygen exchange kinetics between the gas phase and oxide was studied by the oxygen isotope exchange method with gas phase equilibration in the experimental rig [12]. Enriched oxygen ^{18}O , whose fraction was 83.6%, served as a match mark. During the experiment, the changes in concentrations of three mass numbers — C_{32} , C_{34} , C_{36} — were recorded depending on time using a quadrupolar mass-spectrometer Agilent 5973N. The detailed description of the experiment

methodology, evaluation of the inter-phase exchange rate detection accuracy (r_{H} , $\text{atom}\cdot\text{cm}^{-2}\cdot\text{s}^{-1}$) and oxygen diffusion coefficient (D , $\text{cm}^2\cdot\text{s}^{-1}$) has been reported elsewhere [14, 15]. The oxygen interphase exchange rate is numerically equal to the number of oxygen atoms, which exchange at the surface of a unit area per unit of time. The isotope exchange method is one of the few direct methods of oxygen exchange kinetics study, which advantage is a possibility to obtain information

on the oxygen redistribution between a solid oxide and gaseous phase in the adsorption-desorption equilibrium. This allows obtaining high accuracy for the kinetics characteristic values. To compare the obtained values of the interphase exchange rate with the literature data the following translation formula was used:

$$k = r_H \frac{M_r}{(3-\delta)N_A\rho}, \quad (1)$$

where r_H is the oxygen interphase exchange rate ($\text{atom} \cdot \text{cm}^{-2} \cdot \text{s}^{-1}$), k is the oxygen exchange coefficient ($\text{cm} \cdot \text{s}^{-1}$), M_r is the molecular mass, δ is the oxygen non-stoichiometry, N_A is the Avogadro constant, ρ is the sample crystallographic density.

Results and discussion

The oxygen exchange kinetics for the $\text{La}_{0.6}\text{Sr}_{0.4}\text{Co}_{0.8}\text{Fe}_{0.2}\text{O}_{3-\delta}$ oxide was studied at the temperatures of 600–800 °C and the oxygen pressure interval 0.27–2.13 kPa. During the experiment, the changes in ionic current, which correspond to the weight of 32, 34 and 36, versus the exchange time were recorded. Then the obtained values were recalculated into the mass numbers concentrations (see Fig. 5). Typical time dependence for the ^{18}O oxygen isotope fraction changes in a particular experimental condition is presented in Fig. 6. The obtained data can be described using the model developed by Ezin et al. [16] on the basis of the solution suggested by Klier et al. [17].

Fig. 7 illustrates the dependencies of the interphase exchange rate versus oxygen pressure in logarithmic coordinates at different temperatures for the $\text{La}_{0.6}\text{Sr}_{0.4}\text{Co}_{0.8}\text{Fe}_{0.2}\text{O}_{3-\delta}$ oxide. The values of exchange rate increase noticeably as the oxygen pressure and temperature rise. The dependence of interphase exchange rate versus oxygen pressure exhibited a form of the exponential function: $r_H \sim P_{\text{O}_2}^n$. The exponent values that were calculated from the line slopes decreased from 1.03 ± 0.04 down to 0.52 ± 0.03 as the temperature rose.

Boreskov et al. [18] proved that the oxygen exchange occurs at the elevated

temperatures according to the oxygen dissociative adsorption-desorption mechanism for a number of simple oxide systems. In particular, the oxides with equilibrium

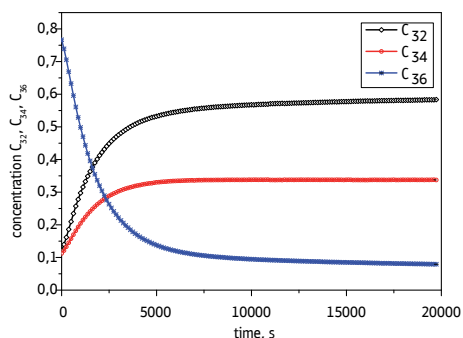


Fig. 5. Experimental concentrations of C_{32} , C_{34} , C_{36} in the gas phase versus time ($T = 800$ °C, $P_{\text{O}_2} = 0.53$ kPa)

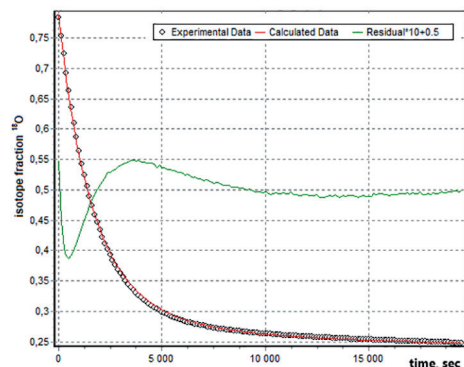


Fig. 6. Fraction of ^{18}O -isotope in the gas phase vs. time in the typical isotope exchange experiment at $T = 800$ °C, $P_{\text{O}_2} = 0.53$ kPa. Points are experimental data, and the line is the fitting result

oxygen concentration do not obey the first type of the exchange mechanism, according to which oxygen atom from the surface does not involved. The isotope exchange proceeds mainly according to the second and third exchange types with the participation of one or two oxygen atoms from the surface. Recently, for the complex oxide systems [15, 19–23] we have demonstrated that the exponents in the equations for the oxygen interphase exchange versus oxygen pressure varies depending on the process which is a rate-determining stage. Often the exchange at high temperature occurs according to the oxygen dissociative adsorption mechanism. Depending on the relation of three exchange types contribution, the oxygen exchange mechanism differs for oxides.

Fig. 8 demonstrates the dependence of the tracer diffusion coefficients of oxygen versus oxygen pressure at various temperatures. The value of the oxygen diffusion coefficient is almost independent of oxygen pressure. Earlier [15] we demonstrated the influence of the oxygen non-stoichiometry on the value of the oxygen tracer diffusion coefficient, for example in lanthanum strontium cobaltites. Almost

constant value of oxygen tracer diffusion coefficient in the Fe-doped lanthanum strontium cobaltite is likely associated with the insignificant changes in the oxygen vacancies concentration within the oxygen pressures range of $0.27 \leq P_{O_2} \leq 2.13$ kPa, which was also confirmed earlier [24–26].

Figs. 9, 10 illustrate the temperature dependencies of oxygen exchange coefficient and oxygen diffusion coefficient, respectively, in comparison with literary data for different oxides [22, 26–29]. The values of activation energy for the exchange and diffusion processes are listed in Table 1. It should be noted that relatively high values of oxygen diffusion and exchange coefficients for the studied $\text{La}_{0.6}\text{Sr}_{0.4}\text{Co}_{0.8}\text{Fe}_{0.2}\text{O}_{3-\delta}$ oxide are comparable with the values for barium praseodymium cobaltite [29] and are greater by the value of magnitude than those for lanthanum strontium manganite [22]. Therefore, it may be assumed that $\text{La}_{0.6}\text{Sr}_{0.4}\text{Co}_{0.8}\text{Fe}_{0.2}\text{O}_{3-\delta}$ is a perspective oxide for the SOFC cathode materials, because of its high values of exponents in the equation for oxygen exchange reaction and good stability in the reducing atmosphere. The substitution of iron for cobalt results in the insignifi-

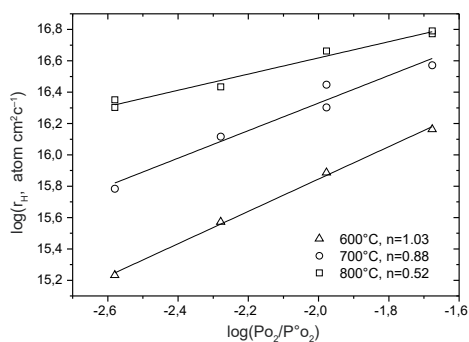


Fig. 7. The oxygen interphase exchange for $\text{La}_{0.6}\text{Sr}_{0.4}\text{Co}_{0.8}\text{Fe}_{0.2}\text{O}_{3-\delta}$ plotted as a function of oxygen partial pressure at different temperatures, $P^{\circ}O_2 = 101.3$ kPa ($n \sim tg\beta$)

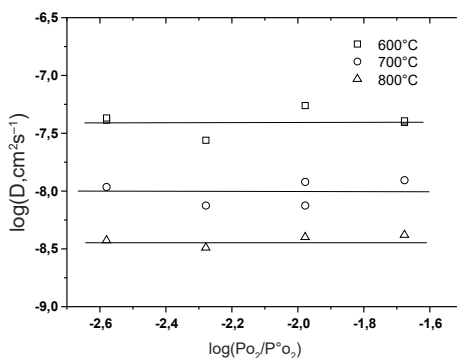


Fig. 8. Oxygen diffusion coefficients versus oxygen partial pressure at different temperatures for the $\text{La}_{0.6}\text{Sr}_{0.4}\text{Co}_{0.8}\text{Fe}_{0.2}\text{O}_{3-\delta}$ oxide

Table 1

The apparent activation energy values for the oxygen surface exchange and oxygen diffusion processes in the mixed conducting oxides

Oxide	Oxygen pressure, kPa	ΔT , °C	Activation energy, eV		Source
			Exchange	Diffusion	
$\text{La}_{0.6}\text{Sr}_{0.4}\text{Co}_{0.8}\text{Fe}_{0.2}\text{O}_{3-\delta}$	2.13	600–800	0.57 ± 0.05	0.92 ± 0.05	This work
$\text{La}_{0.6}\text{Sr}_{0.4}\text{CoO}_{3\pm\delta}$	0.67	600–850	0.11	1.08	[26]
$\text{La}_{0.6}\text{Sr}_{0.4}\text{MnO}_{3\pm\delta}$	0.67	700–850	0.71	1.42	[22]
$\text{Pr}_2\text{NiO}_{4\pm\delta}$	0.67	600–700 700–800	2.0 1.4	2.0	[27]
$\text{La}_2\text{NiO}_{4\pm\delta}$	1.33	600–800	1.38	1.41	[28]
$\text{PrBaCo}_2\text{O}_{6-\delta}$	1.33	600–800	0.76	0.75	[29]

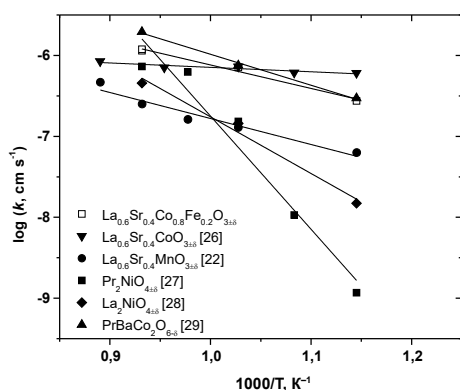


Fig. 9. Temperature dependences of the oxygen exchange coefficient for various mixed conducting oxides

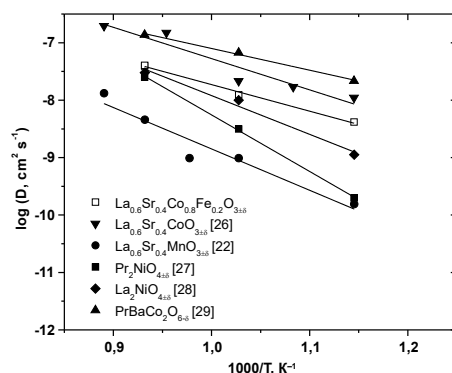


Fig. 10. Temperature dependences of the oxygen tracer diffusion coefficient for various mixed conducting oxides

cant decrease in the oxygen exchange rate; however, its introduction into the cobalt

sublattice increases the stability of oxide in the reducing atmospheres [6].

Conclusions

The oxygen exchange kinetics for the $\text{La}_{0.6}\text{Sr}_{0.4}\text{Co}_{0.8}\text{Fe}_{0.2}\text{O}_{3-\delta}$ oxide was studied using the isotope exchange method with gas phase equilibration. The values of the interphase exchange rate and oxygen diffusion coefficient in $\text{La}_{0.6}\text{Sr}_{0.4}\text{Co}_{0.8}\text{Fe}_{0.2}\text{O}_{3-\delta}$ were calculated. The values of effective ac-

tivation energies for the oxygen interphase exchange and diffusion were calculated.

The exponents in the equations for the oxygen interphase exchange rate were found within the range of 0.52–1.03 at the temperatures of 600–800 °C in the oxygen pressures range of 0.27–2.13 kPa.

Based on these results, it can be concluded that the exchange in the case of $\text{La}_{0.6}\text{Sr}_{0.4}\text{Co}_{0.8}\text{Fe}_{0.2}\text{O}_{3-\delta}$ occurs according to the mechanism of the molecular oxygen dissociative adsorption at the oxide surface.

The obtained results demonstrate that $\text{La}_{0.6}\text{Sr}_{0.4}\text{Co}_{0.8}\text{Fe}_{0.2}\text{O}_{3-\delta}$ possesses high values of oxygen interphase exchange rate and oxygen diffusion coefficient as compared to other oxide materials with mixed conductivity.

Acknowledgements

This work is partly supported by the Russian Science Foundation (Project No. 17-73-10196) using facilities of shared access center "Composition of Compounds" of IHTE UB RAS.

References

1. Petrov AN, Cherepanov VA, Zuyev AY, Zhukovsky VM. Thermodynamic stability of ternary oxides in Ln–M–O systems (Ln = La, Pr, Nd; M = Co, Ni, Cu). *J Solid State Chem.* 1988;77(1):1–14. DOI: 10.1016/0022-4596(88)90083-7.
2. Kharton VV, Figueiredo FM, Kovalevsky AV, Viskup AP, Naumovich EN, Yaremchenko AA, Bashmakov IA, Marques FM. Processing, microstructure and properties of $\text{LaCoO}_{3-\delta}$ ceramics. *J Eur Ceram Soc.* 2001;21(13):2301–9. DOI: 10.1016/S0955-2219(01)00199-6.
3. Yang M, Zhong Y, Liu ZK. Defect analysis and thermodynamic modeling of LaCoO_3 . *Solid State Ionics.* 2007;178(15-18):1027–32. DOI: 10.1016/j.ssi.2007.04.014.
4. Zuev AY, Petrov AN, Vylkov AI, Tsvetkov DS. Oxygen nonstoichiometry and defect structure of undoped and doped lanthanum cobaltites. *Journal of Material Sciences.* 2007;42(6):1901–8. DOI: 10.1007/s10853-006-0345-8.
5. Tai LW, Nasrallah MM, Anderson HU, Sparlin DM, Sehlin SR. Structure and electrical properties of $\text{La}_{1-x}\text{Sr}_x\text{Co}_{1-y}\text{Fe}_y\text{O}_3$. Part 1. The system $\text{La}_{0.8}\text{Sr}_{0.2}\text{Co}_{1-y}\text{Fe}_y\text{O}_3$ // *Solid State Ionics.* 1995;76(3-4):259–71. DOI: 10.1016/0167-2738(94)00244-M.
6. Stevenson JW, Armstrong TR, Carneim RD, Pederson LR, Weber WJ. Electrochemical properties of mixed conducting perovskites $\text{La}_{1-x}\text{M}_x\text{Co}_{1-y}\text{Fe}_y\text{O}_{3-\delta}$ (M = Sr, Ba, Ca). *J Electrochem Soc.* 1996;143(9) 2722–9. DOI: 10.1149/1.1837098.
7. Aksenova TV, Anan'ev MV, Gavrilova LYa, Cherepanov VA. Phase equilibria and crystal structures of solid solutions in the system $\text{LaCoO}_{3-\delta}$ – $\text{SrCoO}_{2.5\pm\delta}$ – $\text{SrFeO}_{3-\delta}$ – $\text{LaFeO}_{3-\delta}$. *Inorg Mater.* 2007;43(3):296–300. DOI: 10.1134/S0020168507030168.
8. Lankhorst MHR, Elshof JE. Thermodynamic quantities and defect structure of $\text{La}_{0.6}\text{Sr}_{0.4}\text{Co}_{1-y}\text{Fe}_y\text{O}_{3-\delta}$ ($y=0-0.6$) from high-temperature coulometric titration experiments. *J Solid State Chem.* 1997;130(2):302–10. DOI: 10.1006/jssc.1997.7378.
9. Choi MB, Lim DK, Wachsmann ED, Song SJ. Oxygen nonstoichiometry and chemical expansion of mixed conducting $\text{La}_{0.1}\text{Sr}_{0.9}\text{Co}_{0.8}\text{Fe}_{0.2}\text{O}_{3-\delta}$. *Solid State Ionics.* 2012;221:22–7. DOI: 10.1016/j.ssi.2012.06.012.
10. Hashimoto S, Fukuda Y, Kuhn M, Sato K, Yashiro K, Mizusaki J. Oxygen nonstoichiometry and thermo-chemical stability of $\text{La}_{0.6}\text{Sr}_{0.4}\text{Co}_{1-y}\text{Fe}_y\text{O}_{3-\delta}$ ($y=0.2, 0.4, 0.6, 0.8$). *Solid State Ionics.* 2010;181(37-38):1713–9. DOI: 10.1016/j.ssi.2010.09.024.

11. Elshof JE, Lankhorst MHR, Bouwmeester HJM. Chemical diffusion and oxygen exchange of $\text{La}_{0.6}\text{Sr}_{0.4}\text{Co}_{0.6}\text{Fe}_{0.4}\text{O}_{3-\delta}$. *Solid State Ionics*. 1997;99(1-2):15–22. DOI: 10.1016/S0167-2738(97)00263-4.
12. Ananyev MV, Kurumchin EKh. Interphase exchange and diffusion of oxygen in lanthanum-strontium cobaltites doped with iron. *Russ J Phys Chem A*. 2010;84(6):1039–44. DOI: 10.1134/S0036024410060269.
13. Bouwmeester HJM, den Otter MW, Boukamp BA. Oxygen transport in $\text{La}_{0.6}\text{Sr}_{0.4}\text{Co}_{1-y}\text{Fe}_y\text{O}_{3-\delta}$. *J Solid State Electrochem*. 2004;8(9):599–605. DOI: 10.1007/s10008-003-0488-3.
14. Kurumchin EKh, Ananjev MV, Vdovin GK, Surkova MG. Exchange kinetics and diffusion of oxygen in systems based on lanthanum gallate. *Russ J Electrochem*. 2010;46(2):205–11. DOI: 10.1134/S1023193510020126.
15. Ananyev MV, Kurumchin EKh, Porotnikova NM. Effect of oxygen nonstoichiometry on kinetics of oxygen exchange and diffusion in lanthanum-strontium cobaltites. *Russ J Electrochem*. 2010;46(7):789–97. DOI: 10.1134/S1023193510070128.
16. Ezin AN, Tsidilkovski VI, Kurumchin EKh. Isotopic exchange and diffusion of oxygen in oxides with different bulk and subsurface diffusivities. *Solid State Ionics*. 1996;84(1-2):105–12. DOI: 10.1016/S0167-2738(96)83012-8.
17. Klier K, Kucera E. Theory of Exchange Reactions between Fluids and Solids with Tracer Diffusion in the Solid. *J Phys Chem Solids*. 1966;27:1087–95. DOI: 10.1016/0022-3697(66)90084-9.
18. Boreskov GK, Kasatkina LA. Catalysis of Isotope Exchange in Molecular Oxygen and Its Application to the Study of Catalysts. *Russ Chem Rev*. 1968;37(8):613–28. DOI: 10.1070/RC1968v037n08ABEH001686.
19. Porotnikova NM, Anan'ev MV, Kurumchin EKh. Effect of Defect Structure of Lanthanum Manganite on Kinetics of Oxygen Exchange and Diffusion. *Russ J Electrochem*. 2011;47(11):1250–6. DOI: 10.1134/S1023193511110139.
20. Anan'ev MV, Bershitskaya NM, Plaksin SV, Kurumchin EKh. Phase equilibriums, oxygen exchange kinetics and diffusion in oxides $\text{CaZr}_{1-x}\text{Sc}_x\text{O}_{3-x/2-\delta}$. *Russ J Electrochem*. 2012;48(9):879–86. DOI: 10.1134/S1023193512090030.
21. Anan'ev MV, Kurumchin EKh, Vdovin GK, Bershitskaya NM. Kinetics of interaction of gas phase oxygen with cerium-gadolinium oxide. *Russ J Electrochem*. 2012;48(9):871–8. DOI: 10.1134/S1023193512090029.
22. Bershitskaya NM, Ananyev MV, Kurumchin EKh, Gavril'yuk AL, Pankratov AA. Effect of oxygen nonstoichiometry on kinetics of oxygen exchange and diffusion in lanthanum-strontium manganites. *Russ J Electrochem*. 2013;49(10):963–74. DOI: 10.1134/S1023193512100047.
23. Wang S, Katsuki M, Dokiya M, Hashimoto T. High temperature properties of $\text{La}_{0.6}\text{Sr}_{0.4}\text{Co}_{0.8}\text{Fe}_{0.2}\text{O}_{3-\delta}$ phase structure and electrical conductivity. *Solid State Ionics*. 2003;159(1-2):71–8. DOI: 10.1016/S0167-2738(03)00027-4.
24. Li Y, Gerdes K, Horita T, Liu X. Surface exchange and bulk diffusivity of LSCF as SOFC cathode: electrical conductivity relaxation and isotope exchange characterizations. *J Electrochem Soc*. 2013;160(4):F343–50. DOI: 10.1149/2.044304jes.

25. Katsuki M, Wang S, Dokiya M, Hashimoto T. High temperature properties of $\text{La}_{0.6}\text{Sr}_{0.4}\text{Co}_{0.8}\text{Fe}_{0.2}\text{O}_{3-\delta}$ oxygen nonstoichiometry and chemical diffusion constant. *Solid State Ionics*. 2003;156(3-4):453–61. DOI: 10.1016/S0167-2738(02)00733–6.
26. Ananyev MV. Izotopnii obmen kisloroda. Teoreticheskie osnovy metoda i ego primeneniye k analizy kinetiki obmena kisloroda s stehiometricheskimi oksidami [Oxygen isotope exchange. Theoretical basis of the method and its application to the analysis of the kinetics of oxygen exchange with non-stoichiometric oxides] Saarbrücken: Lambert Academic Publishing; 2012. 205 p. Russian.
27. Porotnikova NM, Khodimchuk AV, Ananyev MV, Eremin VA, Tropin ES, Farlenkov AS, Pikalova EYu, Fetisov AV. *J Solid State Electrochem*. 2018;22(7):2115–26. DOI: 10.1007/s10008-018-3919-x.
28. Ananyev MV, Tropin ES, Eremin VA, Farlenkov AS, Smirnov AS, Kolchugin AA, Porotnikova NM, Khodimchuk AV, Berenov AV, Kurumchin EK. Oxygen isotope exchange in $\text{La}_2\text{NiO}_{4\pm\delta}$. *Phys Chem Chem Phys*. 2016;18(13):9102–11. DOI: 10.1039/c5cp05984d.
29. Ananyev MV, Eremin VA, Tsvetkov DS, Porotnikova NM, Farlenkov AS, Zuev AYU, Fetisov AV, Kurumchin EK. Oxygen isotope exchange and diffusion in $\text{LnBaCo}_2\text{O}_{6-\delta}$ (Ln = Pr, Sm, Gd) with double perovskite structure. *Solid State Ionics*. 2017;304:96–106. DOI: 10.1016/j.ssi.2017.03.022.